IMATINIB-MESYLATE BLOCKS RECOMBINANT T- TYPE CALCIUM CHANNELS EXPRESSED IN HEK-293 CELLS BY A PTK-INDEPENDENT MECHANISM.

Mauro Cataldi, Annarita Gaudino, Vincenzo Lariccia, Michela Russo[1], Gianfranco di Renzo and Lucio Annunziato

Division of Pharmacology, Department of Neuroscience Federico II, University of Naples, Via Pansini n°5, 80131 Naples, ITALY

JPET Fast Forward. Published on January 12, 2004 as DOI: 10.1124/jpet.103.061184
This article has not been copyedited and formatted. The final version may differ from this version.

Running Title: $Ca_V3.3$ T-type channel blockade by *imatinib-mesylate*

Number of words in the abstract: 250

Number of words in the introduction: 497

Number of words in the discussion: 1401

Number of pages: 28

Number of references: 40

Number of figures: 6

Corresponding Author: Lucio Annunziato, MD
Division of Pharmacology,
Department of Neuroscience,
Federico II University of Naples,
Via Pansini n°5, 80131 Naples, ITALY
Tel.: +33-081-7463318
Fax: +33-081-7463323
e-mail: **lannunzi@unina.it**

Non-standard abbreviarions: CML: chronic myelogenous leukemia; GAERS: genetic absence epilepsy rats of Strasbourg; HVA: high-voltage activated; PDGF: platelet-derived growth factor; PDGFr: platelet-derived growth factor receptor; PTK: protein tyrosine kinase; TEA-Cl: tetraethyl ammonium chloride; VDCC: voltage-dependent calcium channels;

Recommended section of assignment: Cellular and molecular

JPET Fast Forward. Published on January 12, 2004 as DOI: 10.1124/jpet.103.061184
This article has not been copyedited and formatted. The final version may differ from this version.

ABSTRACT

The 2-phenylaminopyrimidine derivative *imatinib-mesylate*, a powerful PTK inhibitor that targets abl, c-kit and the PDGF receptors, is rapidly gaining a relevant role in the treatment of several types of neoplasms. Since first generation PTK inhibitors affect the activity of a large number of voltage-dependent ion channels, the present study explored the possibility that *imatinib-mesylate* could interfere with the activity of T-type channels, a class of voltage-dependent Ca^{2+} channels which take part in the chain of events elicited by PTK activation. The effect of the drug on T-type channel activity was examined using the whole-cell patch-clamp technique with Ba^{2+} (10mM) as the permeant ion in HEK-293 cells, stably expressing the rat $Ca_V3.3$ channels. *Imatinib-mesylate* concentrations, ranging from 30 to 300μM, reversibly decreased $Ca_V3.3$ current amplitude with an IC_{50} of 56.9μM. By contrast, when *imatinib-mesylate* (500 μM) was intracellularly dialyzed with the pipette solution, no reduction in Ba^{2+} current density was observed. The 2-phenylaminopyrimidine derivative modified neither the voltage-dependency of activation nor the steady state inactivation of $Ca_V3.3$ channels. The decrease in extracellular Ba^{2+} concentration from 10 to 2 mM and the substitution of Ca^{2+} for Ba^{2+} increased the extent of 30 μM *imatinib-mesylate*-induced percent channel blockade from 25.9 ± 2.4 to 36.3 ± 0.9 % in 2 mM Ba^{2+} and 44.2 ± 2.3 % in 2mM Ca^{2+}.

In conclusion, *imatinib-mesylate* blocked the cloned $Ca_V3.3$ channels by a PTK-independent mechanism. Specifically, the drug did not affect the activation or the inactivation of the channel but interfered with the ion permeation process.

JPET Fast Forward. Published on January 12, 2004 as DOI: 10.1124/jpet.103.061184
This article has not been copyedited and formatted. The final version may differ from this version.

The 2-phenylaminopyrimidine derivative i*matinib-mesylate* is a remarkable example of a new class of selective protein-tyrosine kinase (PTK) inhibitors that are rapidly gaining a relevant role in the treatment of tumors thanks to their high specificity, potency and good tolerability (Fabbro et al., 2002). *Imatinib-mesylate* is a powerful inhibitor of the PTK *abl*, an enzyme that is pathologically activated in chronic mielogenous leukemia (CML) (Buchdunger et al., 1996; Deininger and Druker, 2003). The drug also blocks *c-kit* and PDGF receptors (PDGFr) (Buchdunger et al., 2000) whose activation seems to be among the major factors promoting the growth of a heterogeneous group of neoplasms including sarcomas, glioblastomas, prostatic cancer, and gastrointestinal tract tumors (Lyseng-Williamson and Jarvis, 2001). More importantly, because of its remarkable activity in CML cases that no longer respond to standard therapies, *imatinib-mesylate* has been approved under accelerated guidelines by the US Food and Drug Administration (FDA) (Arnold K, 2001) and is now considered a relevant achievement in rational drug design and transduction therapy (Capdeville et al., 2002).

Although the block in cell proliferation is the primary pharmacological effect of PTK inhibitors, which explains their promising use in cancer treatment, studies *in vitro* have shown that the first generation of these drugs induce marked changes in cell excitability and ionic homeostasis. The ability of these compounds to affect the activity of a large number of receptor-operated and voltage-dependent ion channels (Davis et al., 2001), such as the L- and N-types of voltage-dependent calcium channels (VDCC) (Cataldi et al., 1996; Wijetunge et al., 2002; Morikawa et al., 1998), partly explains this phenomenon.

The inhibitory action of PTK inhibitors on VDCC could be of special relevance in the case of Low-Voltage Activated (LVA) T-type calcium channels. In fact, these channels, which diverge from HVA channels because of their peculiar permeation and gating properties (Perez-Reyes, 2003; Cataldi et al., 2002), are important functional partners of PTKs, for they cooperate with these

JPET Fast Forward. Published on January 12, 2004 as DOI: 10.1124/jpet.103.061184
This article has not been copyedited and formatted. The final version may differ from this version.

proteins in a number of physiological processes. For example, T-type channels take part in the chain of events leading to cell proliferation and differentiation (Richard and Nargeot, 1996; Kuga et al., 1996) and are essential for the mitogenic response to the PDGF receptors (Wang et al., 1993). Therefore, the ability to block T-type channels could give a PTK inhibitor additional valuable properties that could optimize its pharmacological activity.

Given the relevance of *imatinib-mesylate* as an antineoplastic agent, the present paper explored its potential effect in modifying the activity of T-type channels. In particular, by using the whole-cell patch-clamp technique on HEK-293 cells, stably expressing the recently cloned $Ca_V3.3$ isoform of T-type channels (Lee et al., 1999), specific experimental approaches were adopted to establish whether *imatinib-mesylate* acts on these channels indirectly through a PTK-dependent mechanism, or whether it directly interferes with channel gating or the permeation process. The results showed that *imatinib-mesylate* dose-dependently inhibited the activity of cloned $Ca_V3.3$ channels. However, this effect was not related to PTK inhibition but rather to the drug's interference with the ion permeation process.

JPET Fast Forward. Published on January 12, 2004 as DOI: 10.1124/jpet.103.061184
This article has not been copyedited and formatted. The final version may differ from this version.

METHODS

Cell culture. Stably transfected HEK-293 cells (courtesy of Dr. Perez-Reyes), expressing the rat $Ca_V3.3$ subunit of T-type VDCC (Lee et al., 1999), were cultured in a humidified 5% CO_2 atmosphere using DMEM supplemented with 5% fetal calf serum (FCS), 100 IU/ml penicillin, 100 μg/ml streptomycin, and non-essential aminoacids; they were kept under constant selection with 1g/l geneticin. For electrophysiological recordings, cells were plated on poly-L-lysine (30μg/ml) precoated glass coverslips and used 24-48 hours after plating.

Western Blot Analysis. For western blot analysis confluent $Ca_V3.3$-expressing HEK cells grown onto 100 mm Petri dishes were were collected by scraping and low-speed centrifugation and lysed by shaking at 4°C for 1 hour in a lysis buffer containing, in the case of c-abl, 50 mM Tris-HCl, pH 7.5, 150 mM NaCl, 50 mM NaF, 0.5% Triton X-100, 10% Glycerol, 1 mM PMSF, 1 mM $NaVO_4$ or, in the case of PDGFr, 20 mM Hepes pH 7.4, 50 mM NaF, 1mM sodium azide, 1% triton X-100, 200 μM $NaVO_4$. Both in the case of c-abl and of PDGFr, proteases were blocked adding to the lysis buffer a protease inhibitor cocktail (Complete mini, Roche Diagnostics, Mannheim, Germany) constituted by aprotinin (0.1% final concentration), pepstatin (0.7 mg/mL final concentration) and leupeptin (1 μg/ml final concentration). Samples were cleared by centrifugation and supernatants were used for western blot analysis. Protein concentration was determined using a commercially available kit (Biorad Protein Assay, Biorad Laboratories, Hercules, CA, USA) and 70μg of the total cell lysate were loaded into a 6% polyacrylamide- 0.1% sodium dodecylsulfate (SDS) vertical gel and separated electrophoretically using a Biorad electrophoresis system (Mini-PROTEAN 3 electrophoresis cell, Biorad Laboratories, Hercules, CA, USA). Proteins were then transferred electrophoretically from the gel to a nitrocellulose filter using a Biorad mini-trans blot cell (Biorad Laboratories, Hercules, CA, USA) .

After blocking the non-specific binding sites of nitrocellulose membrane with 5% non-fat dried milk in a Tris Buffer Saline (TBS) solution (20 mM Tris base, 137 mM NaCl, pH7.6 with HCl) additioned with 0.1% Tween-20 for 2 h at room temperature (23 ± 2°C), the filters were incubated for 1 hour at room temperature under constant agitation either with a monoclonal anti-c-abl antibody (1:300 final concentration) (Calbiochem, La Jolla, CA, USA) or a polyclonal anti-PDGFr-β antibody (1:1000 final concentration) (Santa Cruz Biotechnology, Santa Cruz, CA, USA). Total cell lysates from SK-N-BE cells (courtesy of dr. R. Sirabella, Dept. of Neuroscience, Federico II University of Naples) were used as positive controls for anti c-abl blots while, in the case of PDGFr-β detection, total cell lysates obtained from starved IMR-92 fibroblasts after challenging with serum (courtesy of dr. R. Ammendola, Dept. of Biochemistry, Federico II University of Naples) were employed. The antibody-reactive bands were revealed using a commercially available chemiluminescent detection kit using horseradish peroxidase-labelled goat anti-mouse IgG as secondary antibodies (ECL western detection kit, Amersham Pharmacia Biotech, Piscataway, NJ, USA).

Electrophysiology. Experiments were performed by using the whole-cell configuration of the patch-clamp technique. The coverslips, where cells had been cultured, were placed into a laminar flow chamber (Warner Instrument Corporation, Hamden, CT, USA) mounted on the stage of a *Axiovert 25* Zeiss inverted microscope. The cells were continuously superfused by a gravity fed multilane system that allowed the rapid exchange of the perfusing solution. All the experiments were performed at room temperature (23 ± 2 °C).

Ruptured patches were obtained by suction using fire-polished borosilicate electrodes having a final resistance of 3-5 MΩ. The electrodes were back filled with a CsCl-based internal solution containing 110 mM CsCl, 30 mM tetraethyl ammonium chloride (TEA-Cl), 10 mM EGTA, 2 mM $MgCl_2$, 10 mM Hepes, 8 mM Glucose, 15 mM phosphocreatine, 5 mM ATP and 1 mM cAMP (pH 7.4 adjusted with CsOH). Unless otherwise specified, the external solution contained

125 mM N-methyl-D-glucamine, 10 mM $BaCl_2$, 10 mM Hepes and 1 mM $MgCl_2$ (pH 7.4 adjusted with HCl). The osmolarity of the external solution was adjusted to 300 mOsm by adding an appropriate amount of sucrose.

Test pulses were generated and the ensuing currents were collected with an Axon 200 B patch-clamp amplifier (Axon, Union City, CA, USA) driven by the P-Clamp 6 software running on a PC. Currents were filtered at 2 kHz with the amplifier's built-in Bessel filter, and leak currents were subtracted online with a P/4 protocol. Online corrections of membrane capacitance and series resistance were routinely performed by using the specific commands of the amplifier. Data were stored onto the hard disk of the PC. Offline analyses were then performed with the Clampfit 8.0 (Axon, Union City, CA, USA) and Sigmaplot 5.0 (SPSS Inc., Chicago, IL, USA) softwares.

Cell capacitance was calculated upon the integration of current traces generated by cell membrane discharges in response to short (5 ms) square pulses of 5 mV amplitude (from –70 up to –65 mV) which were delivered immediately after rupturing the patch.

Drugs. *Imatinib-mesylate* was a generous gift from Dr. Buchdunger (Novartis, Basel, Switzerland). The drug was dissolved in water as a 10mM stock solution and kept frozen at -20 C until use. Geneticin and ATP-sodium salt were obtained from Calbiochem (LaJolla, CA, USA), whereas CsOH was purchased from Aldrich Chemicals (Milan, Italy). DMEM, FCS, Penicillin, Streptomycin and non-essential aminoacids were purchased from Invitrogen (San Giuliano Milanese, Italy). All the other chemicals were of analytical grade and were purchased from Sigma (Milan, Italy).

Data analysis. All the data have been reported as mean±SEM. Statistical comparisons were performed with ANOVA followed by the Neuman-Keuls post-hoc test. The threshold for statistical significance was set at $p<0.05$. Curve fitting was performed with the Sigma-plot 5.0 (SPSS Inc., Chicago, IL, USA) or the N-fit (The University of Texas, Medical Branch at Galveston, Galveston, Texas, USA) software.

JPET Fast Forward. Published on January 12, 2004 as DOI: 10.1124/jpet.103.061184
This article has not been copyedited and formatted. The final version may differ from this version.

RESULTS

***Imatinib-mesylate* blocks $Ca_V3.3$ channels acting from outside the cell.**

Membrane depolarization, induced by square voltage pulses, elicited large inward currents in $Ca_V3.3$-expressing HEK-293 cells that were bathed with a 10 mM Ba^{2+} solution. These currents displayed all the expected features that clearly differentiated $Ca_V3.3$ channels type from the other cloned members of the Ca_V3 family. In fact, they showed relatively slow kinetics with respect to activation and inactivation (Fig.1A and B). The fact that these currents were blocked by 500 μM Cd^{2+} (Fig.1A), disappeared when Ba^{2+} ions were omitted from the extracellular solution (Fig.1B), and were totally lacking in untransfected HEK-293 cells (Fig.1C), indicated that they were genuine Ba^{2+} currents, flowing through the heterologously expressed T-type channels. Since we were interested in studying the consequences on $Ca_V3.3$ activity of PTK blockade by *imatinib-mesylate*, preliminary experiments were performed to assess whether $Ca_V3.3$-expressing HEK-293 cells do express the PTKs that are inhibited by this drug. Western blot analysis of total cell lysates showed a strong expression of the c-abl protein in this cell line (Fig.1D), while, despite the strong signal observed in positive controls (serum-stimulated IMR-92 fibroblast), no detectable signal was observed when an anti-PDGFr-β antibody was used (data not shown).

Once established that $Ca_V3.3$-expressing HEK-293 cell are an appropriate experimental model, the hypothesis that *imatinib-mesylate* could affect T-type channel activity was explored monitoring the effect of increasing *imatinib-mesylate* concentrations (1 to 300 μM) on Ba^{2+} currents, evoked by square pulse depolarization (from -100 up to 0 mV). Test pulses were delivered with a 10 second interpulse interval to allow the inactivated channels a full recovery from the inactivation and, consequently, to prevent the progressive accumulation of $Ca_V3.3$ channels in the inactive state. *Imatinib-mesylate* induced a marked decrease in current amplitude that was largely reversible upon the drug washout (Fig2A and B). *Imatinib-mesylate*-induced $Ca_V3.3$ blockade was clearly concentration-dependent. Indeed, when the concentration effect curve was fitted to a Hill

function, an estimated IC_{50} of 56.9 μM and a Hill coefficient of 1.27 were obtained (Fig. 2C). Moreover, to rule out the hypothesis that the elevated IC_{50} needed for $Ca_V3.3$ inhibition was due to the poor penetration of the drug inside the cytoplasm, we examined whether 3 and 10 μM concentrations of *imatinib-mesylate*, which were closer to the IC_{50} for PTK inhibition, affected channel activity after an overnight incubation. At both the concentrations tested, *imatinib-mesylate* was unable to reduce the amplitude of Ba^{2+} currents expressed as current density (pA/pF) after the normalization for cell capacitance (Fig. 2D).

Moreover, to see whether the effect of *imatinib-mesylate* on $Ca_V3.3$ channels depended on PTK inhibition (in which case the drug should have acted intracellularly), we examined the impact on channel activity of 500 μM *imatinib-mesylate* concentration dissolved in the pipette solution and dialyzed into the cytoplasm. The results showed that intrapipette *imatinib-mesylate* neither induced a reduction in Ba^{2+} current density at the beginning of the recording (Fig. 3A), nor determined an acceleration in the rate of its spontaneous decrease over a 500 second period (Fig. 3B).

Imatinib-mesylate does not affect $Ca_V3.3$ channel gating, but it interferes with the ion permeation process.

To identify the molecular mechanism responsible for imatinib-*mesylate* effect on $Ca_V3.3$ channels, we examined whether the drug could reduce the ability of the channel to open, in response to a given depolarizing step, or increase its tendency to inactivate at a given membrane potential.

Firstly, the effect of *imatinib-mesylate* on the voltage dependence of Ba^{2+} currents was examined. The delivery of a series of square depolarizing pulses of increasing amplitude elicited inward currents that appeared at membrane potential more positive than –50 mV, reached their maximum around –20 mV, and reverted at approximately +40 mV (Fig. 4A). When the same cells were exposed to 100 μM *imatinib-mesylate* for 180 seconds, the current amplitude was reduced by approximately 70%, at all voltages tested (Fig. 4A). The fact that the drug did not induce marked

JPET Fast Forward. Published on January 12, 2004 as DOI: 10.1124/jpet.103.061184
This article has not been copyedited and formatted. The final version may differ from this version.

changes in the current to voltage (I/V) plots suggested that *imatinib-mesylate*-induced $Ca_V3.3$ channel blockade was not voltage-dependent (Fig. 4B). Given that the voltage-dependence of activation curve tends to spontaneously drift leftward upon prolonged patch-clamping of Ca_V3-expressing HEK-293 cells (Martin et al., 2000), the effect of *imatinib-mesylate* on the voltage-dependence of $Ca_V3.3$ channel activation was determined by the following experiments. I/V plots were obtained from two different groups of cells: one exposed to vehicle and the other to 100 μM *imatinib-mesylate*. No difference in voltage-dependence of activation was observed when the vehicle and *imatinib*-treated cells were compared (V_m= -25.03±0.8 in control and –25.1.3 ± 1.29 in *imatinib-mesylate*-treated cells; k= 5.79±0.6 in control and 5.19±0.4 in *imatinib-mesylate*-treated cells) (Fig. 4C). These results suggested that *imatinib-mesylate* did not reduce the ability of $Ca_V3.3$ channels to open in response to membrane depolarization.

According to the modulated receptor hypothesis of channel blockade (Hondeghem and Katzung, 1984), another mechanism that might determine a reduction in Ba^{2+} current amplitude via an interference with the gating apparatus is the preferential binding of the drug to the inactivated state of the channel and the consequent stabilization of this state.

The percentage of Ba^{2+} currents blocked by *imatinib-mesylate* did not increase with progressive increments in step voltages, as expected from a drug interacting with the inactive state of the channel (Fig. 4D). However, the fact that *imatinib-mesylate*- induced Ba^{2+} current inhibition was not voltage-dependent does not completely exclude the hypothesis that the drug could act on the inactivated state of $Ca_V3.3$ channels. Its binding kinetics could, in fact, be too slow to yield a significant interaction with those channels undergoing inactivation during the short pulses used to generate the I/V plots. To exclude this possibility, the effect of *imatinib-mesylate* on $Ca_V3.3$ channel activity was also studied by analyzing the inward Ba^{2+} currents evoked by step depolarization after long prepulses of increasing voltages. The steady-state inactivation curves, obtained in these conditions, did not differ in those cells exposed to vehicle or to 100 μM *imatinib*-

mesylate (V_m= -57.9 ± 4.4 mV in control and –58.6 ± 4.2 mV in *imatinib*-treated cells; k=7.65 ± 1.5 in control and 11.22 ± 1.3 in *imatinib*-treated cells) (Fig. 5A and B).

Since *imatinib-mesylate* is ionized at physiological pH values, it could interact with fixed negative charges in $Ca_V3.3$ external vestibule, thus interfering with the channel permeation process. This idea can be tested, albeit indirectly, by looking at the impact of changes in extracellular Ba^{2+} concentration on the channel block induced by this 2-phenylaminopyrimidine derivative. In effect, if *imatinib-mesylate* had blocked the $Ca_V3.3$ channels by competing with Ba^{2+} for the access to the pore region, the reduction of Ba^{2+} concentration should have potentiated the drug's blocking activity. To test this hypothesis, cells were bathed in a 2mM Ba^{2+} external solution and repeatedly stepped from –100 up to -20mV before and after the addition of 30μM *imatinib-mesylate*. The ability of 30μM *imatinib-mesylate* to block $Ca_V3.3$ channels was significantly enhanced in a 2mM Ba^{2+} solution. In fact, as opposed to the values recorded before the addition of the drug, Ba^{2+} current amplitude was reduced by 36.3 ± 0.9 and 25.9 ± 2.4 % in 2mM and in 10 mM Ba^{2+} solutions, respectively ($p<0.01$ using ANOVA followed by the Neuman Keuls test) (Fig. 6A, B and D). Since Ca^{2+} is the permeant ion in physiological conditions and a mechanism of channel blockade involving ion permeation could imply a different ability of the drug in blocking Ba^{2+} and Ca^{2+} currents, the effect of 30 μM *imatinib-mesylate* on the inward currents elicited by step depolarization from –100 to –20 mV with 2mM Ca^{2+} in the bath was also assessed. In these experimental conditions, *imatinib-mesylate* induced a 44.2 ± 2.3 % blockade of Ca^{2+} currents, that was significantly different from what observed with 2mM Ba^{2+} ($p<0.05$ using ANOVA followed by the Neuman Keuls test) (Fig. 6C and D).

JPET Fast Forward. Published on January 12, 2004 as DOI: 10.1124/jpet.103.061184
This article has not been copyedited and formatted. The final version may differ from this version.

DISCUSSION

The main findings emerging from the present paper indicated that *imatinib-mesylate* blocks $Ca_V3.3$ T-type channels by acting in a PTK-independent mechanism. Specifically, it interfered with their permeation pathway without affecting the activation or the inactivation of $Ca_V3.3$ channels.

Several arguments support the conclusion that PTK inhibition is not responsible for the T-type channel inhibition exerted by *imatinib-mesylate*. First of all, the IC_{50} for channel blockade was more than 100 times higher than the one needed for PTK inhibition (Buchdunger et al., 1996). This latter result could be explained by the inefficient intracellular diffusion of the drug owing to the short exposure of the cells during the brief patch-clamp experiments. However, the fact that micromolar concentrations of *imatinib-mesylate* were still ineffective when the cells were exposed to the drug for a prolonged time interval clearly excludes this possibility and strongly implies a mechanism that was independent of PTK inhibition. This idea is further supported by the evidence that *imatinib-mesylate* acted from outside the cell and remained ineffective when introduced into the cytoplasm through the recording pipette. As shown by the strong expression of c-abl found in these cell by Western Blot analysis, the lack of efficacy of intrapipette *imatinib-mesylate* cannot be explained with the absence in the cytoplasm of $Ca_V3.3$-expressing HEK-cells of the PTKs susceptible to the blocking action of this drug, and suggests that *imatinib-mesylate* was acting on an extracellular site. In particular, the main factor that determined a decrease in $Ca_V3.3$ channel activity was the drug's reversible binding to an extracellular site that caused the block of the permeation path of the channel itself. Since *imatinib-mesylate* is a charged organic cation, this notion is consistent with the classical evidence, which states that charged drugs and toxins may impinge on the outer vestibule of VDCC and disturb the access of Ba^{2+} ions to the pore region of the channel. The key role played by i*matinib-mesylate* in blocking $Ca_V3.3$ channel ion permeation was highlighted by the experiments performed with low Ba^{2+} concentrations. In fact, when an extracellular solution containing 2 mM Ba^{2+} was used, the extent of *imatinib*-induced $Ca_V3.3$

channel blockade was significantly higher than the one at 10 mM Ba^{2+}. The channel blockade sensitivity to a decrease in the permeant ion concentration was as expected from a drug that competes with Ba^{2+} ions for the access to the pore region of the channel. A further argument supporting the idea that *imatinib-mesylate* exerts its $Ca_V3.3$ channel block activity due to an interference with the permeation process was provided by experiments performed using a 2mM Ca^{2+}-containing extracellular solution. In this experimental conditions the extent of drug-induced channel blockade was significantly higher, clearly suggesting that the nature of the ion competing with *imatinib-mesylate* could determine the effectiveness of the drug-induced channel blockade. Interestingly, Martin et al. (2000) obtained similar findings with the T-type blocker mibefradil that, besides interfering with other channel functions, displays similar permeation-blocking properties. Given a similar mechanism for *imatinib-mesylate*-induced $Ca_V3.3$ channel blockade, a relevant issue that emerges is that of specificity. In fact, it could be argued that, not differently from what observed for mibefradil, this drug could also interact with the pore region of other VDCC channel types. Indeed, preliminary observations from our laboratory confirm this idea since *imatinib-mesylate* proved to be effective also in blocking recombinant L-type channels in stably transfected CHO cells (courtesy of Dr. F. Hofmann, Technische Universitat Munchen, Munich, Germany) coexpressing the rabbit $Ca_V1.2$, β_3 and $\alpha_2\delta$ subunits (Cataldi M., unpublished data).

Contrarily to other T-type channel blockers, *i.e.* mibefradil (McDonough and Bean, 1998; Gomora et al., 2000) and the neuroleptics pimozide and penfluridol (Santi et al., 2002), which do interfere with the channel inactivation process, *imatinib-mesylate* apparently does not. In fact, contrarily to what is expected from drugs that bind to the channel in its inactive state, the extent of channel blockade did not increase despite the progressive increments in the step voltages that increased the inactivation rate of $Ca_V3.3$ channels. Furthermore, the hypothesis that the interaction of the drug with the inactivated state of the channel could be precluded by its slow binding kinetics can also be discarded, since no leftward shift in steady-state inactivation was observed when $Ca_V3.3$ channels were inactivated by long prepulses in the presence of the drug. Similarly, the activation

JPET Fast Forward. Published on January 12, 2004 as DOI: 10.1124/jpet.103.061184
This article has not been copyedited and formatted. The final version may differ from this version.

process seems to be equally unaffected by *imatinib-mesylate*, for this 2-phenylaminopyrimidine derivative did not induce any changes in the channel voltage-dependence of activation.

Therefore, it is worth underscoring the fact that PTK first generation inhibitors (genistein, lavendustin and herbimycin) differ from *imatinib-mesylate*, for they reduce the activity of naïve T-type channels in NG108-15 cells by a PTK-dependent mechanism (Morikawa et al., 1998).

Since T-type channels have a role in a number of physiological processes that are also regulated by the activity of PTKs, such as the control of cell growth (Richard and Nargeot, 1996; Kuga et al., 1996) and neuronal excitability (Perez-Reyes, 2003; Huguenard, 1996), the availability of compounds provided of T-type channel- and PTK-blocking properties could be of valuable clinical interest. For example, a pharmacological approach targeting T-type channels and PTKs simultaneously could be useful to prevent vascular remodelling as it occurrs in arterial hypertension. The rationale behind this approach could be represented by the relevance of both PTKs and T-type channels in the pathogenesis of this condition. In fact, specific PTKs, as the PDGF receptors, which are activated by shear-stress (Hu et al., 1998), contribute to myointimal cell proliferation (Balasubramaniam et al., 2003) and represent the target of novel anti-vascular remodeling therapies (Waltenberger et al., 1999). On the other hand, T-type channels are expressed in proliferating myointimal cells (Kuga et al., 1996; Richard and Nargeot, 1996) and their pharmacological blockade with mibefradil prevents the development of neointimal hyperplasia in spontaneous hypertensive rats (Li and Schiffrin, 1996).

Similarly, the combined blockade of T-type channels and PTKs could also be useful in controlling pathological neuronal excitability, since they are both involved in this process. Specifically, T-type channels play a relevant role in regulating neuron excitability (Perez-Reyes, 2003; Huguenard, 1996) and take part in the process of epileptogenesis. The crucial involvement of T-type channels in seizures is, in fact, demonstrated by the finding that the antiseizure drug etosuximide blocks these channels (Coulter et al., 1990; Gomora et al, 2001) and by the observation that the thalamic neurons of genetic absence epilepsy rats of Strasbourg (GAERS), an experimental

JPET Fast Forward. Published on January 12, 2004 as DOI: 10.1124/jpet.103.061184
This article has not been copyedited and formatted. The final version may differ from this version.

model of absence epilepsy, show higher T-type current density than average (Tsakiridou et al., 1995). By contrast, $Ca_V3.1$ T-type channel knock-out mice have shown to be resistant to thalamic spike-and-wave discharges, normally induced by the administration of $GABA_B$ receptor agonists (Kim et al., 2001). The involvement of PTKs in the process of epileptogenesis is supported by the evidence that specific PTKs, such as PYK-2, are activated in response to seizures (Tian et al., 2000) and by the fact that the overexpression of selected PTK, such as Fyn (Kojima et al., 1998), raises the tendency to develop seizures *in vivo*, whereas the knocking-out of the same kinases has opposite effects (Cain et al., 1995). Furthermore, the susceptibility of hippocampal slices *in vitro* to epileptic discharges, in response to electrical stimulation, can be raised by adding the PTK *src* into the recording pipette and can be decreased with the use of the *src* inhibitor PP2 (Sanna et al, 2000). Therefore, a drug that can simultaneously block T-type channels and specific PTKs could constitute a promising antiseizure agent.

Lastly, since T-type channels are selectively expressed in proliferating tumor cells, whereas their expression is lost after cell differentiation (Hirooka et al., 2002; Mariot et al., 2002), it has been suggested that they are also involved in tumor growth. Although it is still matter of controversy, this hypothesis suggests that T-type channel blockade could synergize with PTK inhibition and consequentely determine an antineoplastic effect. Actually, drugs provided with T-type blocking properties such as mibefradil and pimozide have already shown to exert an antiproliferative effect on retinoblastoma and breast cancer cell lines *in vitro* (Bertolesi et al., 2002).

In conclusion, *imatinib-mesylate* has the ability to block $Ca_V3.3$ channels by a PTK-independent mechanism when used in the high micromolar range. More importantly, its T-type channel blocking ability could add to this important drug additional and useful pharmacological properties that could be exploited in the development of a new class of derivatives, which in addition to having the capability of blocking T-type channels could also retain the remarkable PTK-inhibitory properties of *imatinib-mesylate*.

JPET Fast Forward. Published on January 12, 2004 as DOI: 10.1124/jpet.103.061184
This article has not been copyedited and formatted. The final version may differ from this version.

ACKNOWLEDEGMENTS

The authors are indebted to Dr. Ed Perez-Reyes (Department of Pharmacology, University of Virginia, Charlottesville, VA) for kindly providing the stably transfected HEK-293 cells and to Dr. Elisabeth Buchdunger (Novartis Pharma, Basel, Switzerland) for the generous gift of imatinib-mesylate.

Special thanks to Dr. Maurizio Taglialatela for the critical reading of the manuscript, to Dr. Tommaso Russo and Dr. Nicola Zambrano for their enlightening discussions on the data and to Dr R. Ammendola and R. Sirabella for their help in performing anti PDGFr-β Western Blot analysis.

The authors would also like to express their appreciation to Dr. Paola Merolla and to Mrs. Marcella Donato for the editorial help and to Mr. Vincenzo Grillo for his technical support in performing the experiments.

REFERENCES

Arnold K (2001) After 30 years of laboratory work, a quick approval for STI571. *J Natl Cancer Inst* 93**:** 972.

Balasubramaniam V, Le Cras TD, Ivy DD, Grover TR, Kinsella JP and Abman SH (2003) Role of platelet-derived growth factor in vascular remodeling during pulmonary hypertension in the ovine fetus. *Am J Physiol Lung Cell Mol Physiol* 284: L826-L833.

Bertolesi GE, Shi C, Elbaum L, Jollimore C, Rozenberg G, Barnes S and Kelly ME (2002) The Ca^{2+} channel antagonists mibefradil and pimozide inhibit cell growth via different cytotoxic mechanisms. *Mol Pharmacol* 62**:** 210-219.

Buchdunger E, Zimmermann J, Mett H, Meyer T, Muller M, Druker BJ and Lydon NB (1996) Inhibition of the Abl protein-tyrosine kinase in vitro and in vivo by a 2-phenylaminopyrimidine derivative. *Cancer Res* 56:100-104.

Buchdunger E, Cioffi CL, Law N, Stover D, Ohno-Jones S, Druker BJ and Lydon NB (2000) Abl protein-tyrosine kinase inhibitor STI571 inhibits in vitro signal transduction mediated by c-kit and platelet-derived growth factor receptors. *J Pharmacol Exp Ther* 295(1):139-145.

Cain DP, Grant SG, Saucier D, Hargreaves EL and Kandel ER (1995) Fyn tyrosine kinase is required for normal amygdala kindling. *Epilepsy Res* 22**:** 107-114.

Capdeville R, Buchdunger E, Zimmermann J and Matter A (2002) Glivec (STI571, imatinib), a rationally developed, targeted anticancer drug. *Nat Rev Drug Discov* 1**:** 493-502.

Cataldi M, Perez-Reyes E and Tsien RW (2002) Differences in apparent pore sizes of low and high voltage-activated Ca^{2+} channels. *J Biol Chem* 277**:** 45969-45976.

Cataldi M, Taglialatela M, Guerriero S, Amoroso S, Lombardi G, Di Renzo G and Annunziato L (1996) Protein-tyrosine kinases activate while protein-tyrosine phosphatases inhibit L-type calcium channel activity in pituitary GH3 cells. *J Biol Chem* 271**:** 9441-9446.

Coulter DA, Huguenard JR and Prince DA (1990) Differential effects of petit mal anticonvulsants and convulsants on thalamic neurones: calcium current reduction. *Br J Pharmacol* 100:800-806.

Davis M, Wu X, Nurkiewicz TR, Kawasaki J, Gui P, Hill MA and Wilson E (2001) Regulation of ion channels by protein tyrosine phosphorylation. *Am J Physiol Heart Circ Physiol* 281**:** H1835-H1862.

Deininger MW and Druker BJ (2003) Specific targeted therapy of chronic myelogenous leukemia with imatinib. *Pharmacol Rev* 55:401-423.

Fabbro D, Parkinson D and Matter A (2002). Protein tyrosine kinase inhibitors: new treatment modalities? *Curr Opin Pharmacol* 2**:** 374-381.

Gomora JC, Xu L, Enyeart JA and Enyeart JJ (2000) Effect of mibefradil on voltage-dependent gating and kinetics of T-type Ca(2+) channels in cortisol-secreting cells. *J Pharmacol Exp Ther* 292:96-103.

Gomora JC, Daud AN, Weiergraber M and Perez-Reyes E (2001) Block of cloned human T-type calcium channels by succinimide antiepileptic drugs. Mol Pharmacol. 60:1121-1132.

Hirooka K, Bertolesi GE, Kelly ME, Denovan-Wright EM, Sun X, Hamid J, Zamponi GW, Juhasz AE, Haynes LW and Barnes S (2002) T-Type calcium channel alpha1G and alpha1H subunits in human retinoblastoma cells and their loss after differentiation. *J Neurophysiol* 88**:** 196-205.

Hondeghem LM and Katzung BG (1984) Antiarrhythmic agents: the modulated receptor mechanism of action of sodium and calcium channel-blocking drugs. *Annu Rev Pharmacol Toxicol* 24**:** 387-423.

Huguenard JR (1996) Low threshold calcium current in central nervous system neurons. *Annu Rev Physiol* 58:329-348

Hu Y, Bock G, Wick G and Xu Q (1998) Activation of PDGF receptor alpha in vascular smooth muscle cells by mechanical stress. *FASEB J* 12**:** 1135-1142.

Kim D, Song I, Keum S, Lee T, Jeong MJ, Kim SS, McEnery MW and Shin HS (2001) Lack of the burst firing of thalamocortical relay neurons and resistance to absence seizures in mice lacking alpha(1G) T-type Ca^{2+} channels. *Neuron* 31:35-45.

Kojima N, Ishibashi H, Obata K and Kandel ER (1998) Higher seizure susceptibility and enhanced tyrosine phosphorylation of N-methyl-D-aspartate receptor subunit 2B in fyn transgenic mice. *Learn Mem* 5**:** 429-445.

Kuga T, Kobayashi S, Hirakawa Y, Kanaide H and Takeshita A (1996). Cell cycle-dependent expression of L- and T-type Ca^{2+} currents in rat aortic smooth muscle cells in primary culture. *Circ Res* 79**:** 14-19.

Lee JH, Daud AN, Cribbs LL, Lacerda AE, Pereverzev A, Klockner U, Schneider T and Perez-Reyes E (1999) Cloning and expression of a novel member of the low voltage-activated T-type calcium channel family. *J Neurosci* 19**:** 1912-1921.

Li JS, Schiffrin EL (1996) Effect of calcium channel blockade or angiotensin-converting enzyme inhibition on structure of coronary, renal, and other small arteries in spontaneously hypertensive rats. J Cardiovasc Pharmacol 28:68-74.

Lyseng-Williamson K and Jarvis B (2001) Imatinib. *Drugs* 61**:** 1765-1774.

Mariot P, Vanoverberghe K, Lalevee N, Rossier MF and Prevarskaya N (2002) Overexpression of an alpha 1H (Cav3.2) T-type calcium channel during neuroendocrine differentiation of human prostate cancer cells. *J Biol Chem* 277**:** 10824-10833.

Martin RL, Lee JH, Cribbs LL, Perez-Reyes E and Hanck DA (2000) Mibefradil block of cloned T-type calcium channels. *J Pharmacol Exp Ther* 295**:** 302-308.

McDonough SI and Bean BP (1998) Mibefradil inhibition of T-type calcium channels in cerebellar purkinje neurons. *Mol Pharmacol* 54:1080-1087.

Morikawa H, Fukuda K, Mima H, Shoda T, Kato S and Mori K (1998) Tyrosine kinase inhibitors suppress N-type and T-type Ca^{2+} channel currents in NG108-15 cells. *Pflugers Arch* 436**:** 127-132.

Perez-Reyes E (2003) Molecular physiology of low-voltage-activated t-type calcium channels. *Physiol Rev* 83**:** 117-161.

Randall AD and Tsien RW (1997) Contrasting biophysical and pharmacological properties of T-type and R-type calcium channels. *Neuropharmacology* 36:879-893.

Richard S and Nargeot J (1996) T-type calcium currents in vascular smooth muscle cells: a role in cellular proliferation? *In Low-Voltage-Activated Channels* (Tsien RW, Clozel JP and Nargeot J eds) pp 123-132 ADIS, Chester.

Sanna P, Berton F, Cammalleri M, Tallent MK, Siggins GR, Bloom FE and Francesconi W (2000) A role for Src kinase in spontaneous epileptiform activity in the CA3 region of the hippocampus. *Proc Natl Acad Sci U S A*, 97**:** 8653-8657.

Santi CM, Cayabyab F, Sutton KG, McRory JE, Mezeyova J, Hamming KS, Parker D, Stea A and Snutch TP (2002) Differential inhibition of T-type calcium channels by neuroleptics. *J Neurosci*, 22: 396-403

Tian D, Litvak V and Lev S (2000) Cerebral ischemia and seizures induce tyrosine phosphorylation of PYK2 in neurons and microglial cells. *J Neurosci* 20**:** 6478-6487.

Tsakiridou E, Bertollini L, de Curtis M, Avanzini G and Pape HC (1995) Selective increase in T-type calcium conductance of reticular thalamic neurons in a rat model of absence epilepsy. *J Neurosci* 15:3110-3117.

Waltenberger J, Uecker A, Kroll J, Frank H, Mayr U, Bjorge JD, Fujita D, Gazit A, Hombach V, Levitzki A and Bohmer FD (1999). A dual inhibitor of platelet-derived growth factor beta-receptor and Src kinase activity potently interferes with motogenic and mitogenic responses to PDGF in vascular smooth muscle cells. A novel candidate for prevention of vascular remodeling. *Circ Res*, 85: 12-22.

Wang Z, Estacion M and Mordan LJ (1993) Ca^{2+} influx via T-type channels modulates PDGF-induced replication of mouse fibroblasts. *Am J Physiol* 265: C1239-C1246.

Wijetunge S, Dolphin AC and Hughes AD (2002) Tyrosine kinases act directly on the alpha1 subunit to modulate Ca(v)2.2 calcium channels. *Biochem Biophys Res Commun* 290**:** 1246-1249.

Woodhull AM (1973) Ionic blockage of sodium channels in nerve. *J Gen Physiol* 61:687-708.

FOOTNOTES

This work was supported by the following grants to L.A.: MIUR COFIN 2001, from the Ministero Italiano per l' Università e la Ricerca Scientifica); FIRB 2002 RBNE01E7YX_007, POP and Legge 41 form Regione Campania; Programma Speciale art. 12bis comma 6, d. Igs 229/99 form ministero della Salute and Regione Campania.

Reprint requests should be addressed to Lucio Annunziato, MD, Division of Pharmacology, Department of Neuroscience, Federico II University of Naples, Via Pansini n°5, 80131 Naples, ITALY

1. M.R. is a Ph. D. student recipient of a fellowship grant from E.T.I. (Ente Italiano Tabacchi).

JPET Fast Forward. Published on January 12, 2004 as DOI: 10.1124/jpet.103.061184
This article has not been copyedited and formatted. The final version may differ from this version.

LEGENDS TO FIGURES

Figure 1. **Barium currents and c-abl expression in $Ca_V3.3$ expressing HEK-293 cells**. *Panel A* and *B* show the inward currents elicited by a series of depolarizing steps in two different $Ca_V3.3$ expressing HEK-293 cells, bathed, on the left, with a 10 mM Ba^{2+} solution and, on the right, after a 3 minute perfusion, with a 10mM Ba^{2+} solution containing 500 μM Cd^{2+} (panel A) or a 120 mM N-methyl-D-Glucamine Ba^{2+} free solution (panel B). Membrane potential was held at –90 mV, and 75 ms square pulses of increasing voltages (from –60 up to 30 mV in 10 mV increments) were delivered with a 10 second interpulse interval. *Panel C* reports the currents that were recorded with a similar depolarization protocol in an untransfected HEK 293 cell bathed with a 10 mM Ba^{2+} solution. The traces reported in panels A, B and C of the figure are representative of at least five other cells of each group recorded with the same experimental conditions. In *Panel D* a western blot performed using an anti c-abl antibody on total cell lysates from $Ca_V3.3$-expressing HEK-293 cells (left lane) and from human neuroblastoma SK-N-BE cells (right lane) is shown. 70 μg of proteins per lane have been loaded. See methods for further details.

Figure 2. **Imatinib-Mesylate blocks $Ca_V3.3$ channels.** *Panel A* shows the effect of 100 μM *imatinib-mesylate* on Ba^{2+} currents elicited by repeated step depolarization to 0 mV. The panel reports three superimposed current traces obtained in a representative cell taken from a group of five cells. The first trace was obtained during the baseline perfusion with 10 mM Ba^{2+}, the second at the nadir of Ba^{2+} current, during 100 μM *imatinib-mesylate* perfusion, and the third during the drug washout. The cells were held at –90 mV, and, as shown in the inset, Ba^{2+} currents were evoked by square pulse depolarizations (75ms in duration) from –100mV up to 0 mV, delivered at a 10 second interval. Cells were perfused with a 10mM Ba^{2+} solution and, after 50 seconds of baseline recording, the perfusion was switched to a Ba^{2+}solution containing 100 μM *imatinib-mesylate*. The

cells were perfused with *imatinib-mesylate* for 250 seconds. The drug was, then, washed out by switching back the perfusion to the 10 mM Ba^{2+} solution. *Panel B* shows the time-course of maximal inward Ba^{2+} currents in the same cell. Each plotted data point represents the maximal current value recorded in response to each of the consecutive voltage steps delivered according to the above-reported protocol. *Panel C* shows the concentration-effect curve generated with the step depolarization protocol described above and different *imatinib-mesylate* concentrations (1-300 μM). Different groups of cells were exposed to the different *imatinib-mesylate* concentrations. Each data point represents the mean±SEM of percentage decrease referred to the maximal inward current induced by each *imatinib-mesylate* concentration as compared with the values recorded before drug addition. The number of cells in each group is reported in the Figure. The values have been fitted using the Hill equation $y=max/(1+(x/IC_{50})^n)$ where y is the inhibition of Ba^{2+} currents expressed as percentage of baseline current amplitude, max is the maximal inhibition, x is the *imatinib-mesylate* concentration in the bathing solution, and n is the Hill coefficient. *Panel D* reports the mean±SEM of Ba^{2+} current densities recorded in $Ca_V3.3$ expressing cells that were exposed to an overnight incubation with 3 or 10 μM *imatinib-mesylate* and in their respective controls. The values were obtained by averaging the maximal values of the amplitude of inward barium currents, that were evoked in each cell of each experimental group by a series of 5 consecutive voltage steps (from –100 to 0 mV, holding potential=-90 mV, interpulse interval= 10 seconds). The currents were normalized to the cell capacitance, extrapolated from the integration of the capacitative currents, which were elicited by brief subthreshold voltage steps (as detailed in the "*Methods"* section). Statistical significance has been assessed with the two tail Student's t-test for unpaired data.

Figure 3. *Imatinib-mesylate* does not block $Ca_V3.3$ channels when dialyzed into the cytoplasm through the patch pipette. *Panel A* shows the mean±SEM of the Ba^{2+} current densities measured immediately after reaching the whole cell configuration and after correcting for the membrane

capacitance in a group of 6 cells patched with standard intracellular solution and in a group of 6 cells patched with a 500 μM *imatinib-mesylate* containing intracellular solution. *Panel B* reports the time course of maximal current densities recorded in response to a series of square pulse depolarizations in the same two groups of cells of panel A. Each data point is the mean±SEM of the values recorded in the six cells of each group. As reported in the inset, $Ca_V3.3$ channels were activated by delivering a series of 75 ms steps (from –100 up to 0 mV) with an interpulse interval of 10 seconds. Current densities were obtained by normalizing to cell capacitance (expressed in pF and calculated as reported in the *Methods* section) the maximal Ba^{2+} current amplitudes obtained in response to each step depolarization.

Figure 4. Effect of *imatinib-mesylate* on the voltage-dependence of Ba^{2+} currents in $Ca_V3.3$-expressing HEK-293 cells. *Panel A* shows the Ba^{2+} currents elicited by a series of depolarizing square pulses of increasing voltage, that were delivered to the same cell before and after a 180 second perfusion of 100μM *imatinib-mesylate*. Membrane potential was held at –90mV and a square pulse was delivered every 10 seconds. The step voltage was increased from –60 to +30 mV in consecutive 10mV increments. The depicted cell is representative of a group of eight. *Panel B* reports the current to voltage (I/V) plot generated by the data collected in the same 8 cells before and after the exposure to *imatinib-mesylate*. The data were normalized and expressed as percentage of the maximal inward current (I_{max}) recorded in the absence of the drug. *Panel C* shows the *voltage-dependence of activation* curves generated from the I/V plots. The I/V plots were obtained with a protocol similar to the one reported in Fig.4A in a group of 7 cells exposed to vehicle for 180 seconds before patching, and in another group exposed to 100 μM *imatinib-mesylate* for the same amount of time. The graph shows the mean±SEM of the ratios (expressed as a function of step voltages) between the conductance calculated for each step (G) and the maximal conductance attained in the whole experiment (G_{max}). Both values obtained in the presence and in the absence of

the drug are reported. Conductance was estimated as the ratio between the I_{max}, reached in response to each step, and the driving force that was calculated as the difference between the voltage of the step and the reversal potential (E-Erev) (Randall and Tsien, 1997). The values were fitted to the equation $G/G_{max}= 1/(1-e^{(Vm-V)/k})$ (where V is the voltage of the depolarizing pulse, V_m is the midpoint of activation, and k is the voltage step needed to induce an increase of e-times in whole cell conductance [e is the base of natural logarithms]). *Panel D* reports the fractional blockade of Ba^{2+} currents induced by *imatinib-mesylate* expressed as a function of step voltages. For each voltage, Ba^{2+} currents recorded in the presence *imatinib-mesylate* were expressed as the percentage of the one detected before drug addition. To exclude any significant interference of channel activation, the analysis was restricted to voltages higher than –20 mV, since a constant number of channels can be assumed to be opened by the voltage step when the saturation of the voltage activation curve is reached (Woodhull, 1973).

Figure 5. Lack of effect of *imatinib-mesylate* on the steady-state inactivation of Ba^{2+} currents in $Ca_V3.3$-expressing HEK-293 cells.

Panel A shows the steady-state inactivation curves obtained in two groups of five cells, one bathed with 10 mM Ba^{2+} and the other exposed to a 100 μM *Imatinib*-containing Ba^{2+} solution. The current traces, obtained in a representative cell of each group, are reported in *panel B*. Steady-state inactivation curves were generated using the protocol described in the inset of panel B. In particular, $Ca_V3.3$ channels were inactivated by applying a series of long (5 seconds) prepulses of increasing amplitude (from –100 to +20 mV in 10mV increments). The amount of ion channels still available for opening at the end of the prepulse was estimated by looking at the amplitude of the inward currents elicited by a brief depolarizing step up to 0 mV, delivered 5ms after setting the membrane potential back to the holding potential value. Each data point is the mean±SEM of the maximal inward Ba^{2+} currents recorded in each cell during each step depolarization up to 0 mV. The data points were fitted to the Boltzman function $I_{Ba}=(I_{max}/(1+e^{(Vm-V)/k})$, where I_{Ba} is the

amplitude of the inward Ba^{2+} current recorded after each step; I_{max} is the maximum value of inward Ba^{2+} current amplitude, reached during the entire experiments; V_m is the midpoint of inactivation; and k is the voltage needed to reduce e-times the amplitude of inward Ba^{2+} current amplitude (where e is the basis of natural logarithms).

Figure 6. Effect on *imatinib*-induced $Ca_V3.3$ blockade of replacing Ca^{2+} for Ba^{2+} ions or changing Ba^{2+} concentration in the extracellular solution. *Panel A, B* and *C* show representative current traces obtained in three different $Ca_V3.3$-expressing HEK-cells bathed with an extracellular solution containing either 10 mM Ba^{2+} (panel A) or 2 mM Ba^{2+} (panel B) or 2 mM Ca^{2+} (panel C). As shown in the inset, currents were elicited by a series of 75ms step depolarizations, from -100 to -20 mV, delivered with a 10 second interpulse interval. For each cell, we reported a current trace acquired during the baseline perfusion with a drug-free extracellular solution, a current trace obtained at the nadir of 30 μM *imatinib*-induced current decrease, and a current trace recorded during the drug washout. The inset of each panel reports the time-course of maximal inward current amplitude obtained in the respective cell. The traces reported in panels *A*, *B* and *C* of the figure are representative of at least five other cells for each group recorded with the same experimental conditions. In *Panel D* the mean±SEM of the percent decreases in inward current amplitude induced by 30 μM *imatinib*-mesylate respect to the values recorded before the addition of the drug attained in each of the three experimental groups are compared. The single asterisk indicates $p<0.05$ vs 2 mM Ba^{2+} while the double asterisk indicates $p<0.01$ vs 10 mM Ba^{2+}.

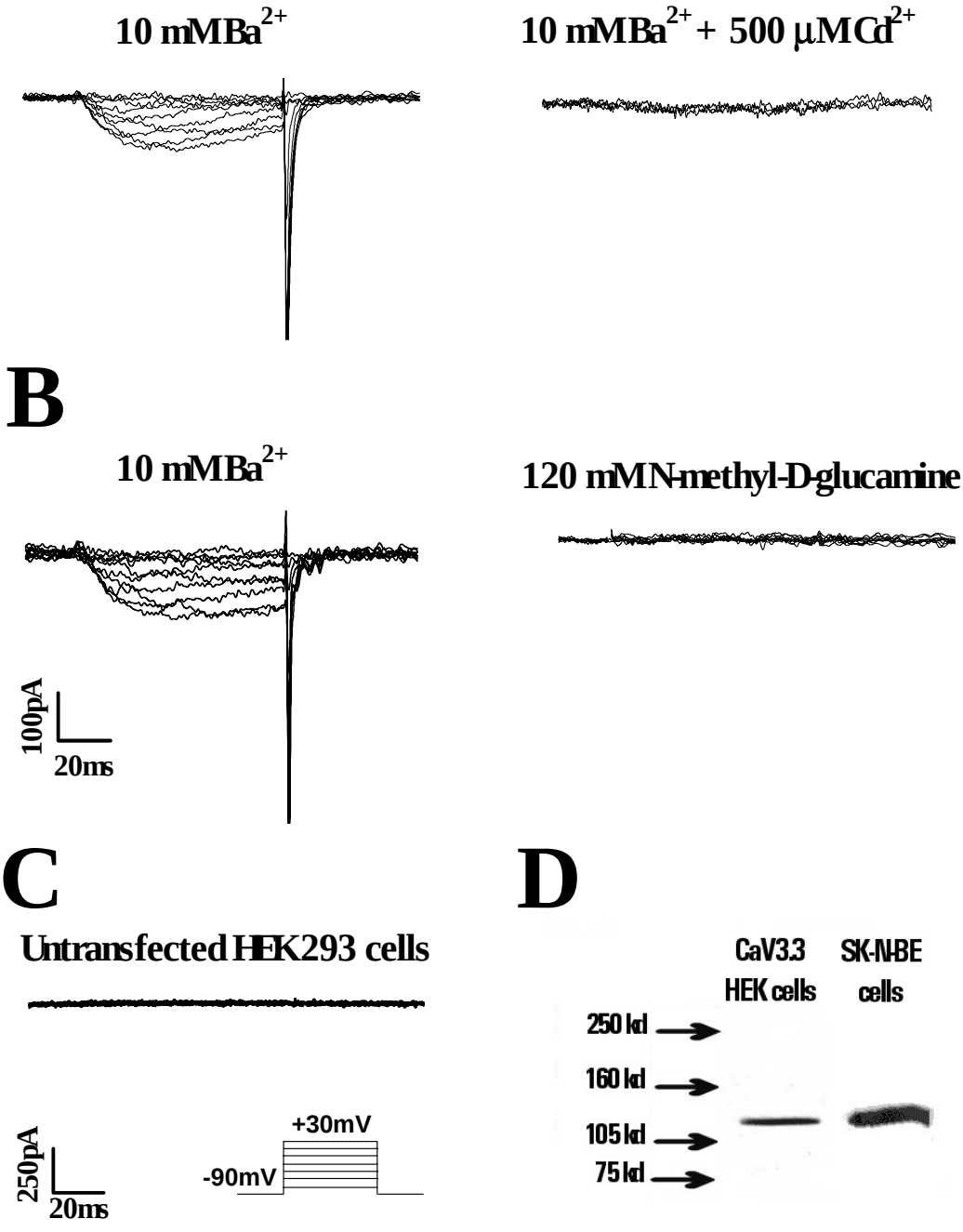

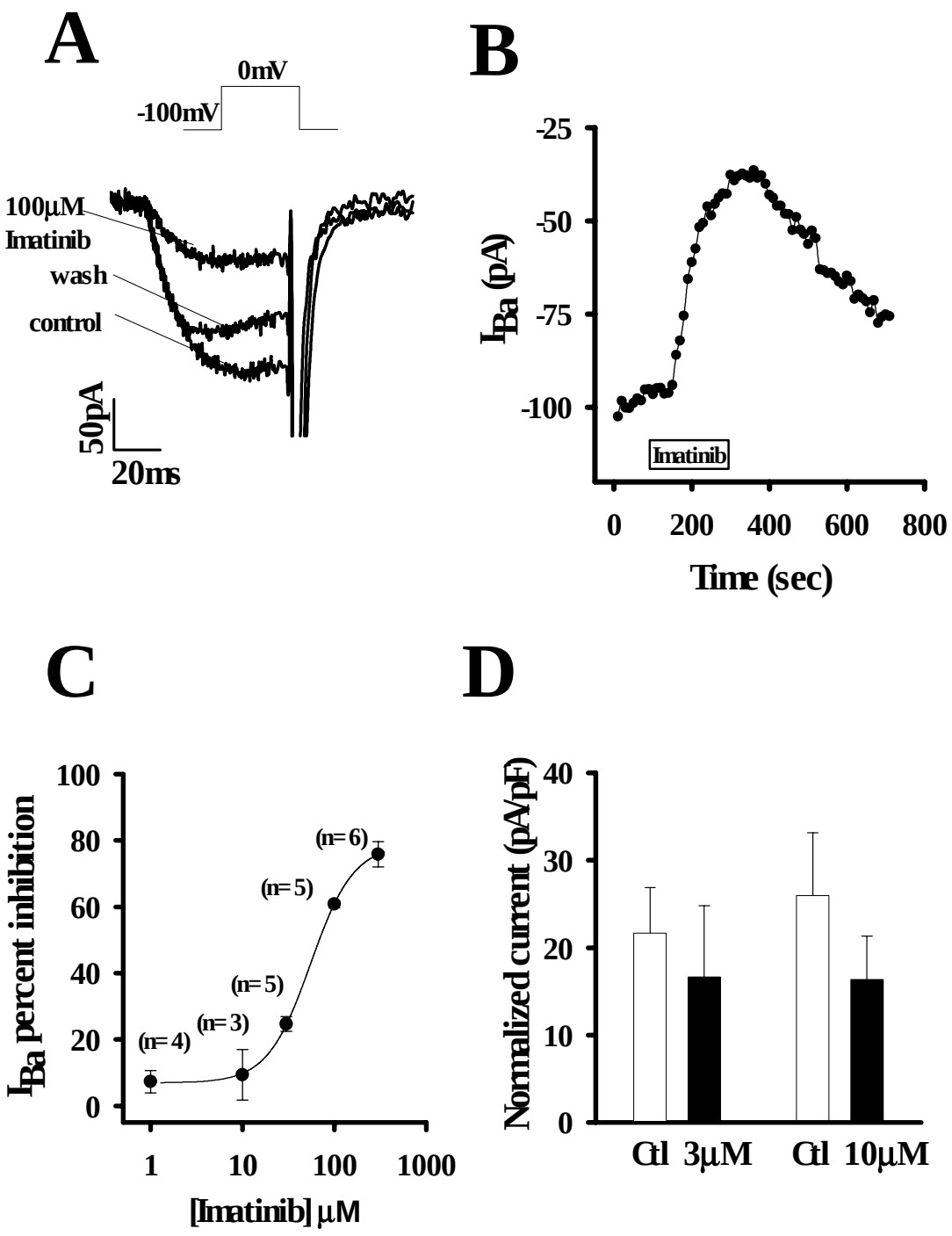

Cataldi et al., Fig. 2

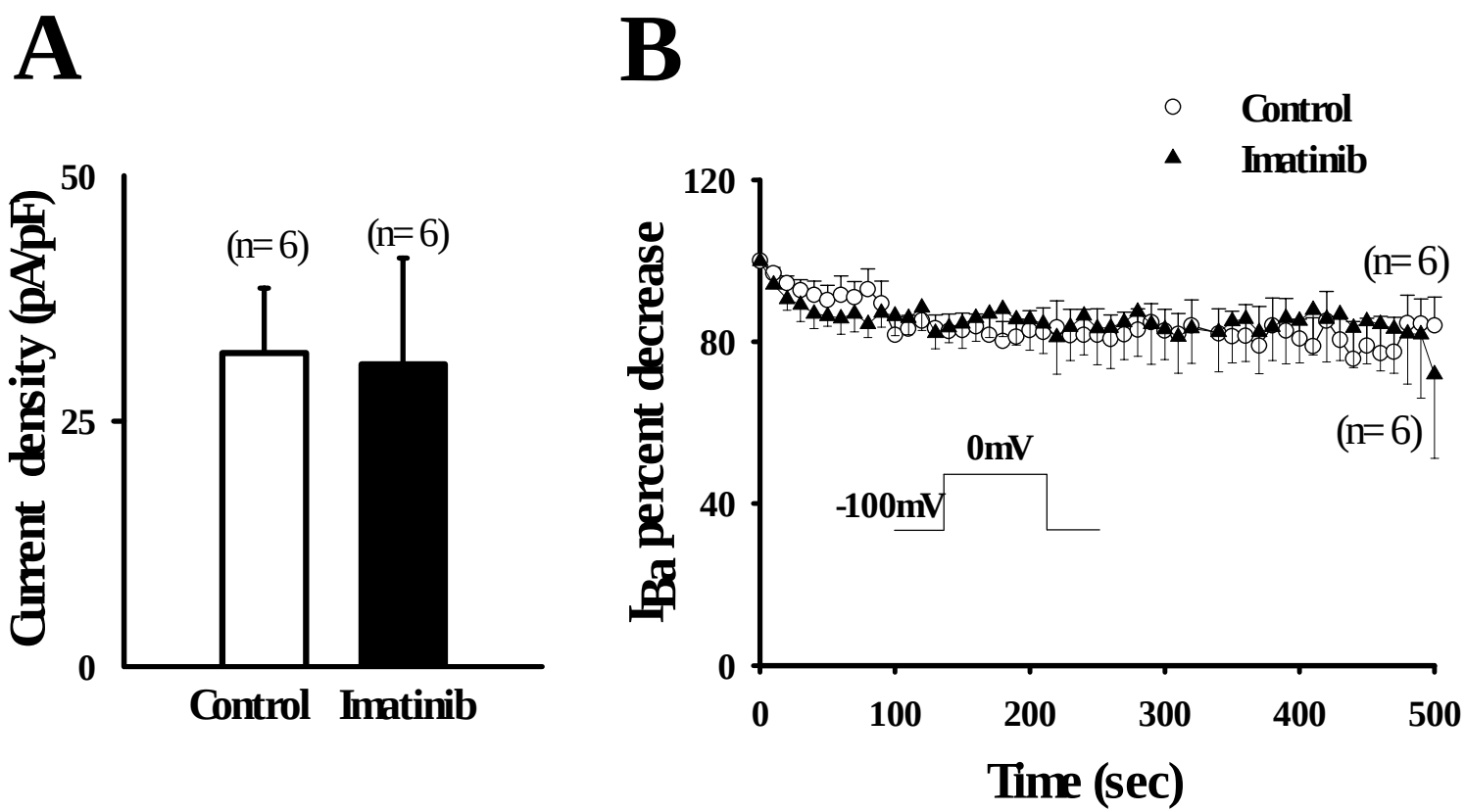

Cataldi et al., Fig. 3

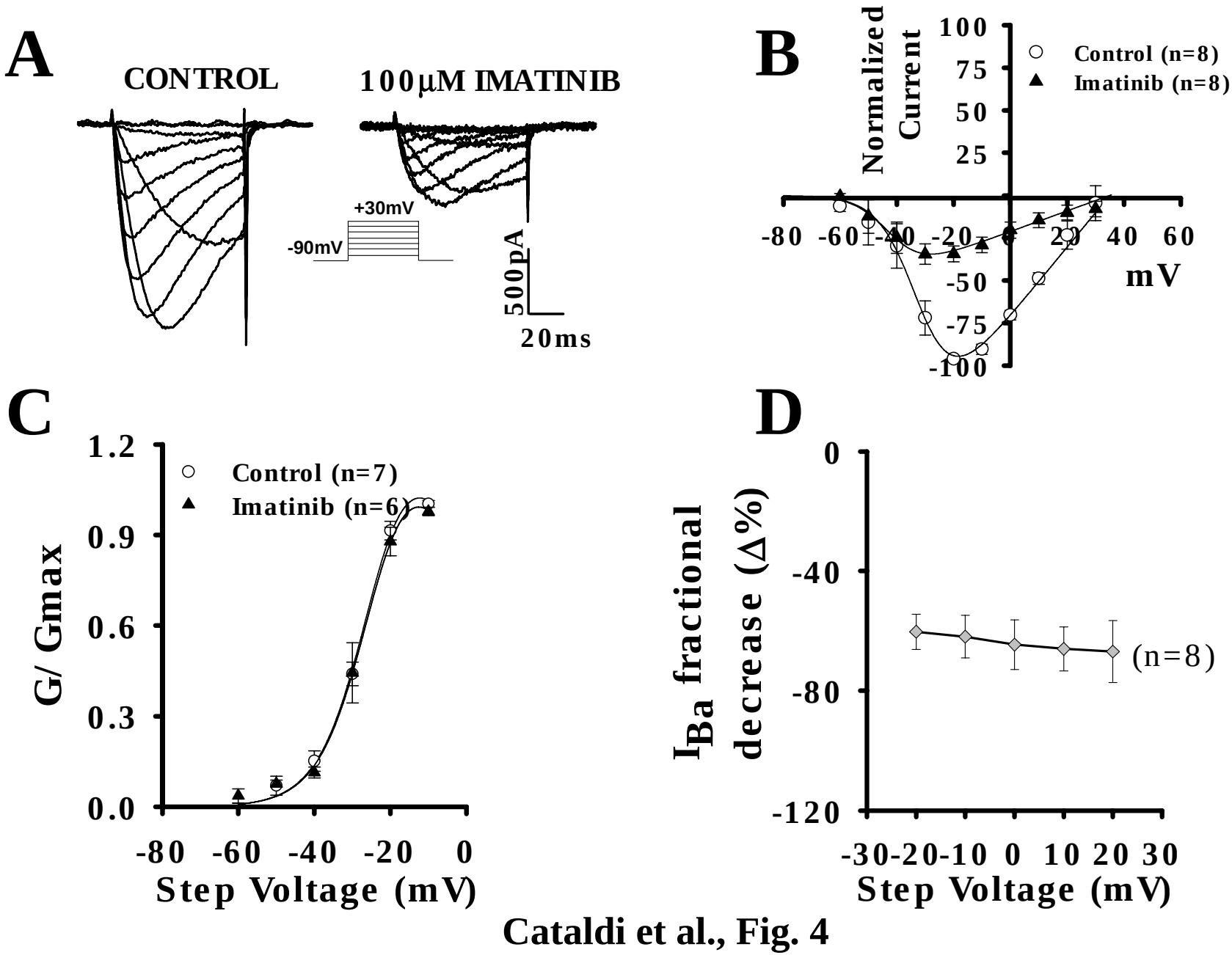

Cataldi et al., Fig. 4

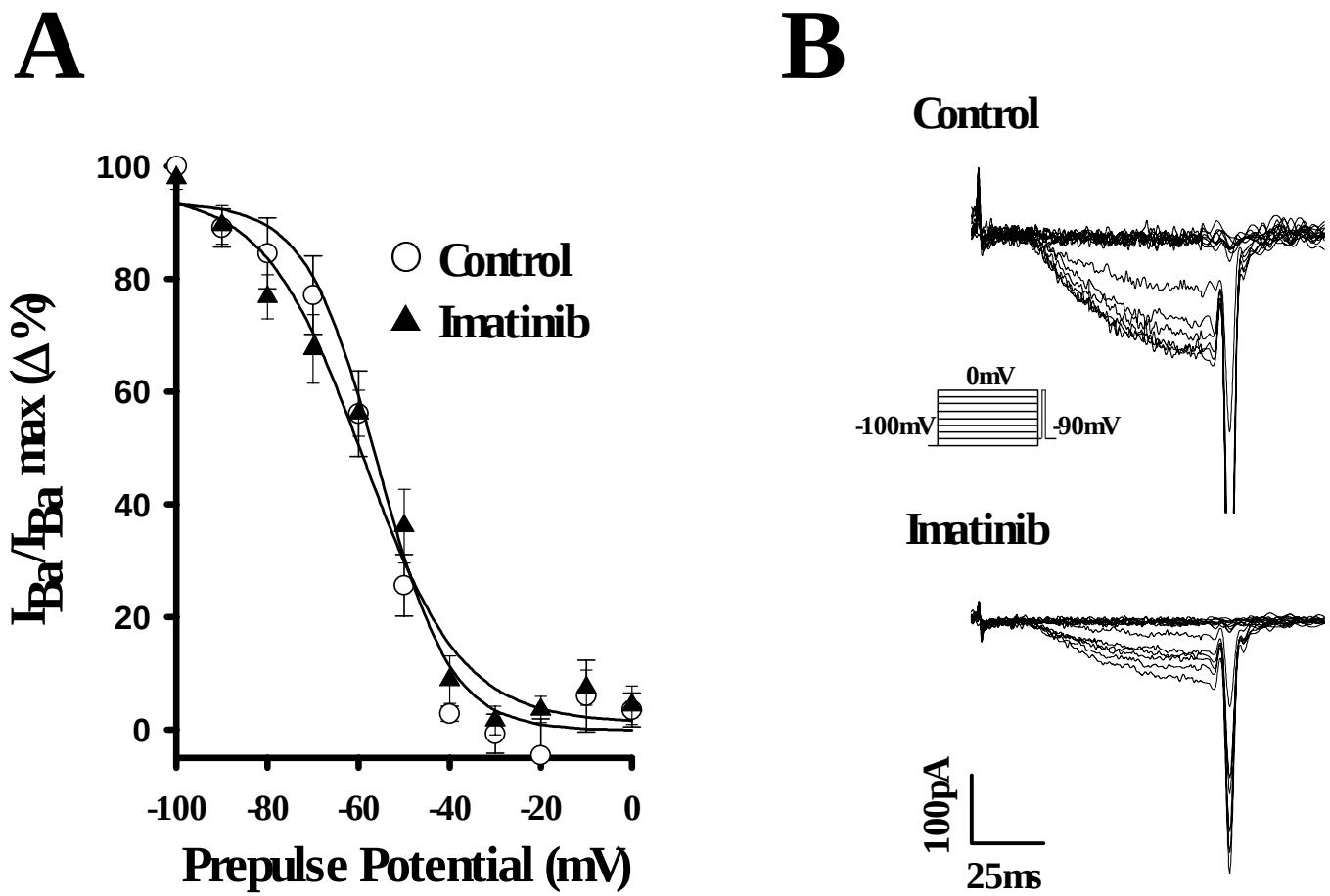

Cataldi et al., Fig. 5

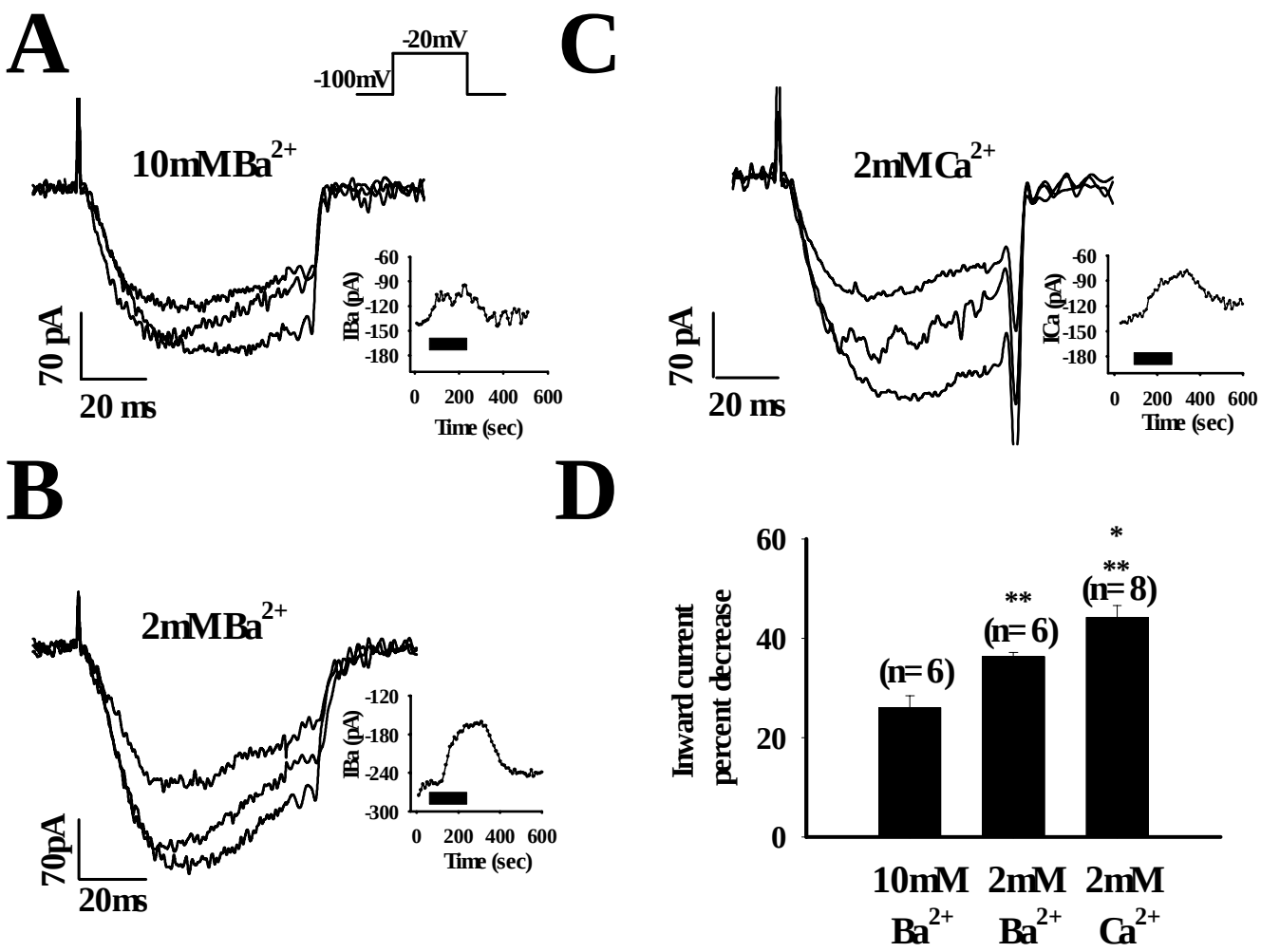

Cataldi et al., Fig. 6